J Solid State Electrochem (2001) 5: 495–501
DOI 10.1007/s100080100227

ORIGINAL PAPER

M. Lurdes F. Ciríaco · M. Isabel da Silva Pereira
Manuel R. Nunes · M. Helena Mendonça
Fernanda M. Costa

Preparation and characterization of $KTa_{0.9}Fe_{0.1}O_{3-\delta}$ perovskite electrodes

Received: 3 September 2000 / Accepted: 16 May 2001 / Published online: 21 July 2001

Abstract The effect of the partial substitution of tantalum by iron on the structural and electrical properties of the $KTaO_3$ perovskite-type oxide powders has been studied. The powders were prepared by the standard ceramic method, and the respective structural characterization performed by X-ray powder diffraction. From the synthesized oxide samples, iron-coated electrodes were fabricated and tested as the anode for the oxygen evolution reaction in alkaline medium. An estimation of the electrode's capacity has been calculated from the charging currents and the corresponding roughness factor evaluated. The electrocatalytic activity/stability of the oxide electrodes in alkaline solutions has been analysed through the kinetic parameters.

Keywords Perovskite oxides · Oxygen evolution · Anode material

Introduction

The scope of the application of photoelectrochemistry is very broad, especially in the areas of environmental clean-up and electrosynthesis. One of the main goals is no doubt the discovery of stable, non-polluting and cheaper photoactive polycrystalline materials to be used as photoelectrodes. Tantalates are potential candidates; particularly, single crystals of $KTaO_3$ perovskite are referred to as stable and efficient photoanodes for the photoassisted electrolysis of water in concentrated alkaline solutions [1, 2]. $KTaO_3$ is an n-type semiconductor presenting an ideal cubic perovskite structure with a lattice parameter $a = 0.3989$ nm [3]. A value of 3.5 eV is reported for the band gap of the reduced oxide [4]. In practical applications, materials with lower band gaps are required.

Changes in the oxide solid-state properties are possible by the introduction of foreign cations in the perovskite structure. Bockris and Otagawa [5, 6, 7] carried out a systematic study on several substituted perovskites in an attempt to correlate their surface structure and electrocatalytic properties in oxygen evolution from alkaline solutions. In our laboratory we have shown that drastic changes are observed in the electrical properties as well as in the electrochemical behaviour of the perovskite system $BaSn_{1-x}Sb_xO_3$ ($0 \le x \le 0.17$), when tin is partially replaced by antimony [8, 9, 10]. In the $KTaO_3$ perovskite structure, Cu^{2+}, Co^{2+}, Mn^{2+} and Fe^{3+} species can be introduced to replace the Ta^{5+} metal ion, constituting acceptors [11]. EPR studies have shown that, under appropriate conditions of oxygen partial pressure, Fe^{3+} can be oxidized to Fe^{4+} or reduced to Fe^{2+}, Fe^{3+} being in general the dominant species [11]. Electron holes dominate the electrical conduction of samples treated in atmospheres of high O_2 pressure.

In this work we report the synthesis of polycrystalline powder samples with nominal composition $KTa_{0.9}Fe_{0.1}O_{3-\delta}$, derived from the $KTaO_3$ perovskite by the partial replacement of tantalum by iron. This substitution was carried out to search for effects on the oxide physicochemical properties and consequently on its electrochemical behaviour, having in mind possible applications as photoanodes. The powder oxides were prepared by the ceramic route and characterized by XRD and SEM/EDS. From the powders, coated iron electrodes were prepared and tested as oxygen anode materials in alkaline solutions.

Presented at the international conference "Solid State Chemistry 2000", 3–8 September 2000, Prague, Czech Republic

M. Isabel da Silva Pereira (✉) · Manuel R. Nunes
M. Helena Mendonça · Fernanda M. Costa
Departmento de Química e Bioquímica,
Centro de Ciências Moleculares e Materiais,
Faculdade de Ciências, Universidade de Lisboa,
Campo Grande, 1749-016 Lisboa, Portugal
E-mail: misp@fc.ul.pt
Tel.: +351-21-7500109
Fax: +351-21-7500088

M. Lurdes F. Ciríaco
Departamento de Química da Universidade de Beira Interior,
6201-001 Covilhã, Portugal

Experimental

Synthesis of the powder samples

The $KTa_{0.9}Fe_{0.1}O_{3-\delta}$ oxide powders were prepared by the conventional ceramic method by heating, in air, stoichiometric amounts of K_2CO_3 (99.9%, Merck), Fe_2O_3 (99%, Merck) and Ta_2O_5 (99.9%, Fluka) in an alumina boat. The reaction mixture was ground carefully in an agate mortar, pelleted and heated in a muffle furnace. Intermediate regrindings were done during the synthesis to ensure homogeneity. In order to test the effect of the final heat treatment on the oxide features, two synthesis temperatures were used. A first set of samples was heated at 973 K during 48 h and the second one heated at 973 K for 24 h, followed by a second heating at 1373 K for another 24 h. As a reference material, samples of $KTaO_3$ were also prepared under the same conditions as the iron-containing oxides.

The progress of the reaction was monitored by X-ray powder diffraction analysis.

Electrode preparation

The $Fe/KTa_{0.9}Fe_{0.1}O_{3-\delta}$ coated electrodes were prepared by brush-painting an iron disk support (99.5%, Goodfellow, 15 mm in diameter and 1.02 mm thick) with a homogenized oxide suspension on Triton X-100 (Merck). After each application, the solvent was evaporated and the dried layer fired for 5 min in a pre-heated oven at 673 K [12]. This operation was repeated until the desired oxide loading (5 ± 1 mg cm^{-2}) was reached. The electrodes were finally annealed at the same temperature for 1 h.

Before use the iron disks were mechanically polished with emery paper, dipped in a diluted HCl solution for 30 min and finally rinsed with plenty of water.

Electrochemical measurements

All the electrochemical measurements were carried out in a three-compartment glass cell, at room temperature, using a Tacussel potentiostat/galvanostat (model PJT 35-2, interface IMT-1). The working electrode was the $Fe/KTa_{0.9}Fe_{0.1}O_{3-\delta}$ disk, which fitted into a polypropylene holder. All potentials were measured against a commercial saturated Ag/AgCl reference electrode and the auxiliary electrode was a platinum foil. The solutions were prepared volumetrically from Millipore water and pro analysis reagents, and deareted with nitrogen, before each experiment.

Characterization techniques

The powder and electrode samples were structurally characterized by X-ray diffraction, using a Philips PW 1710 X-ray diffractometer, with Cu-Kα radiation ($\lambda = 0.15418$ nm) and automatic data acquisition with APD Philips (v. 3.5B) software.

SEM images were obtained with a Hitachi scanning electron microscope (model S-2700) for both powders and electrodes, and EDS analysis was carried out with an Oxford model 60-74 detector for X-ray analysis with a beryllium window.

Electrical resistivity measurements were performed on sintered pellets, in the range 773–973 K, using the Van der Pauw four-probe method, with platinum contacts.

Iron, potassium and tantalum contents were also determined by chemical analysis.

Results

Characterization of the powder samples and electrodes

Structural characterization

Figure 1 shows the XRD patterns for the $KTa_{0.9}Fe_{0.1}O_{3-\delta}$ oxide powders synthesized at the final synthesis temperatures of 973 and 1373 K. The patterns are similar to the ones obtained for the $KTaO_3$ samples prepared under the same conditions. The XRD data indicate, for both temperatures, a perovskite phase presenting a cubic unit cell in accordance with the literature. The d spacing and h,k,l values for $KTaO_3$ and $KTa_{0.9}Fe_{0.1}O_{3-\delta}$ oxide samples are presented in Table 1, where the values for the perovskite phase in JCPDS file

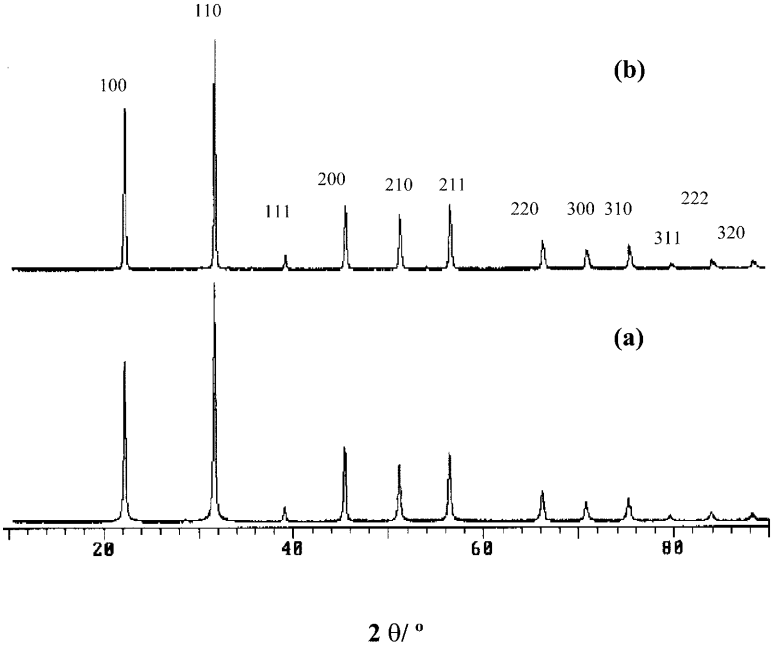

Fig. 1 X-ray diffractograms for the $KTa_{0.9}Fe_{0.1}O_{3-\delta}$ powder samples synthesized at 973 K (**a**) and 1373 K (**b**)

Table 1 *d* spacing and *h*,*k*,*l* values for $KTaO_3$ and $KTa_{0.9}Fe_{0.1}O_{3-\delta}$ oxide samples

h k l	*d* ($KTaO_3$) (Å)			*d* ($KTa_{0.9}Fe_{0.1}O_{3-\delta}$) (Å)	
	$T = 1373$K[a]	$T = 973$K	$T = 1373$K	$T = 973$K	$T = 1373$K
1 0 0	3.9885	3.9850	3.9958	3.9895	3.9771
1 1 0	2.8208	2.8207	2.8260	2.8229	2.8147
1 1 1	2.3036	2.3019	2.3090	2.3044	2.2999
2 0 0	1.9948	1.9948	1.9991	1.9954	1.9923
2 1 0	1.7841	1.7850	1.7886	1.7850	1.7824
2 1 1	1.6286	1.6286	1.6324	1.6295	1.6273
2 2 0	1.4106	1.4107	1.4102	1.4118	1.4093
3 0 0	1.3296	1.3301	1.3296	1.3272	1.3288
3 1 0	1.2614	1.2615	1.2614	1.2624	1.2607
3 1 1	1.2027	1.2032	1.2024	1.2035	1.2020
2 2 2	1.1514	1.1523	1.1516	1.1519	1.1510
3 2 0	1.1064	1.1062	1.1063	1.1067	1.1061

[a]JCPDS file no. 38-1470

no. 38-1470 are also included. The X-ray pattern and data for the samples prepared at 1373 K present very weak lines corresponding to the $KTaO_3$ cubic phase modification that occurs at that temperature according to JCPD 35-1036. Table 2 presents the calculated lattice parameters and, for comparison, the published value for the perovskite phase in JCPDS file no. 38-1470.

Figure 2 shows the X-ray diffraction patterns for the electrodes, obtained immediately following the electrode preparation and after use as oxygen evolution anodes. The pattern for the iron support is also presented. The data show that the perovskite phase is always present. However, the lines of the support are already visible for the electrodes used.

SEM/EDS studies

The morphology of the surface and bulk of the sintered pellets was examined by SEM and Fig. 3a and b illustrates the size distribution and homogeneous aggregation of the crystallites of the sintered $KTa_{0.9}Fe_{0.1}O_{3-\delta}$ oxide phase obtained at 973 K. A grain size around 0.5 μm is observed. No significant differences were observed for the samples synthesized at 1373 K.

EDS data were used to calculate the oxide Fe/Ta atomic ratio. The experimental values are average values obtained from six measurements, three on the surface and three on an internal surface. All these measurements gave similar values, indicating that the samples are chemically homogeneous. The calculated values are in accordance with the expected ones from the stoichiometry and are reported in Table 3. Chemical analysis of potassium, tantalum and iron was also performed and gave similar results to the EDS data, as Table 3 shows.

The electrode's surface was examined by SEM (Fig. 3c) and the coating thickness estimated. A value

Table 2 Lattice parameters for the $KTaO_3$ and $KTa_{0.9}Fe_{0.1}O_{3-\delta}$ oxide powders

Sample	T_s (K)	$a = b = c$ (nm)
$KTaO_3$[a]	1373	0.3989
$KTaO_3$[b]	973	$0.3990 \pm 0.3822\times10^{-4}$
$KTaO_3$[b]	1373	$0.3989 \pm 0.1745\times10^{-4}$
$KTa_{0.9}Fe_{0.1}O_{3-\delta}$	973	$0.3991 \pm 0.2703\times10^{-4}$
$KTa_{0.9}Fe_{0.1}O_{3-\delta}$	1373	$0.3986 \pm 0.4540\times10^{-4}$

[a]CPDS file no. 38-1470
[b]Prepared under the same conditions as the $KTa_{0.9}Fe_{0.1}O_{3-\delta}$ samples

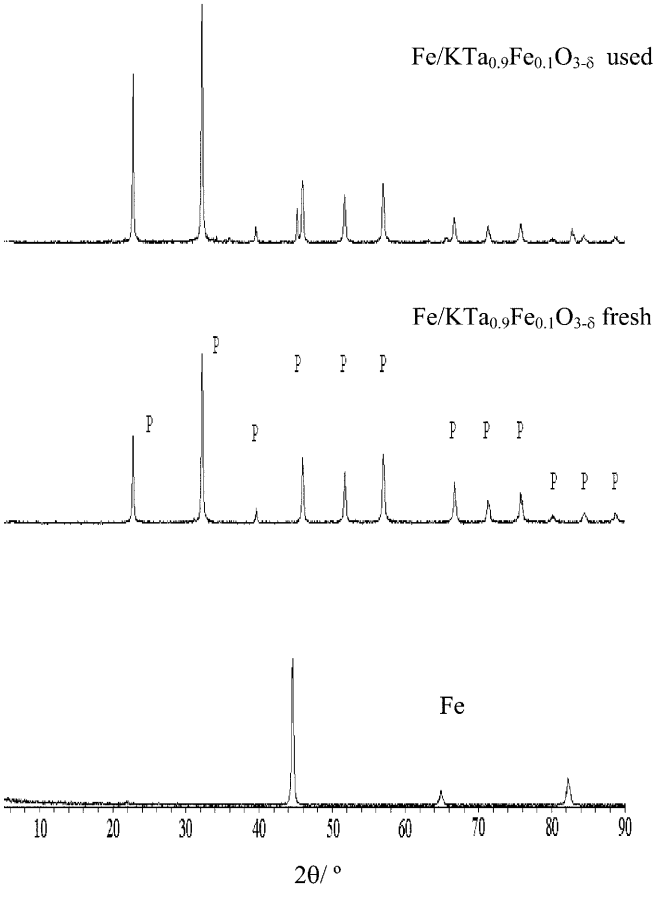

Fig. 2 X-ray diffractograms for fresh and used $Fe/KTa_{0.9}Fe_{0.1}O_{3-\delta}$ electrodes. The X-ray diffractogram for the iron support is also included

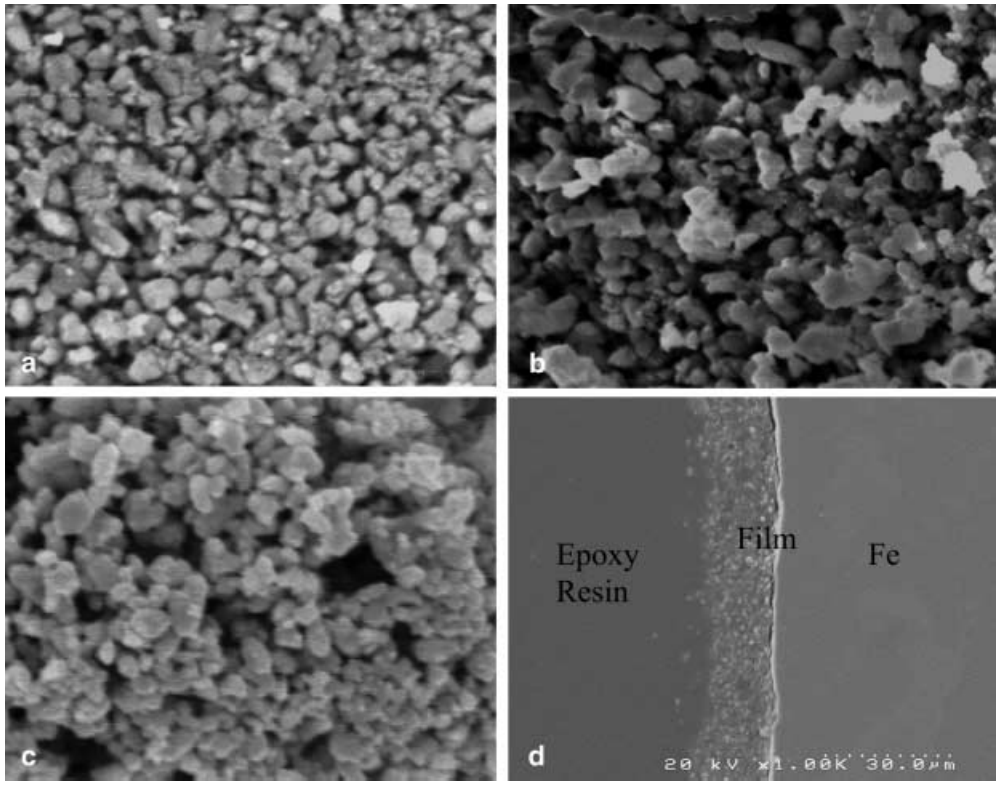

Fig. 3 SEM for a sintered $KTa_{0.9}Fe_{0.1}O_{3-\delta}$ pellet: surface, ×5000 (**a**); fracture surface, ×5000 (**b**); and for the coated oxide electrode: surface, ×5000 (**c**); cross section (**d**)

around 16 µm was obtained for fresh electrodes (Fig. 3d). Small losses on the coating are observed for the electrodes used, which is in accordance with the XRD pattern obtained for those electrodes.

Electrical behaviour

Electrical conductivity measurements were carried out in the temperature range 773–973 K. The thermal dependence of the electrical conductivity for the $KTaO_3$ and iron-substituted oxides present no significant difference for the two sets of samples, prepared at temperatures of respectively 973 and 1373 K, as Fig. 4 shows. Semiconductor behaviour is always observed, with very high resistivity values for the whole samples. Values varying from 10^6 to 10^7 Ω cm were obtained at 773 K. The lower resistivity values were obtained for the samples containing iron, synthesized at 1373 K. From the Arrhenius plots, the activation energies of conduction were obtained. The corresponding evaluated values of the band gap are presented in Table 4. For the samples containing Fe the E_{gap} presents a value of 2.5 eV, approaching the 2 eV reported by Lee et al. [13] for iron-doped $KTaO_3$ samples and lower than the 3.5 eV reported for the $KTaO_3$ oxide [4].

Table 3 Fe/Ta atomic ratio for the $KTa_{0.9}Fe_{0.1}O_{3-\delta}$ oxide samples

Analysis type	T_s (K)	$Fe/Ta_{theoretical}$	$Fe/Ta_{experimental}$
Chemical	973	0.11	0.11
Chemical	1373	0.11	0.11
EDS	973	0.11	0.09
EDS	1373	0.11	0.12

Voltammetric studies

Electrochemical characterization of the perovskite $Fe/KTa_{0.9}Fe_{0.1}O_{3-\delta}$ electrodes was performed in

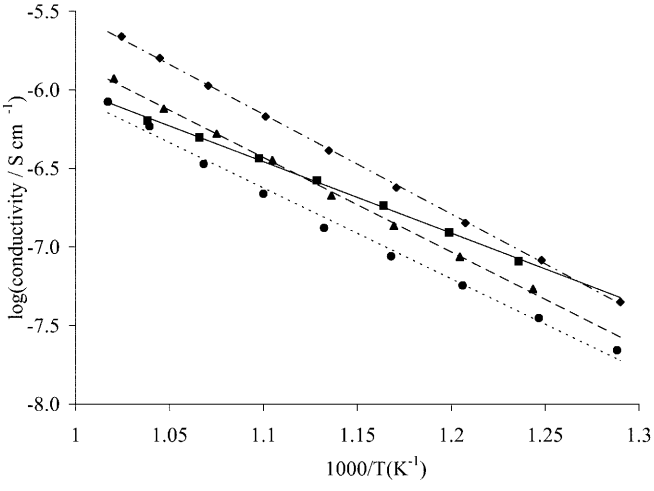

Fig. 4 Thermal dependence of the electrical conductivity of $KTaO_3$ (■, $T_s = 973$ K; ●, $T_s = 1373$ K) and $KTa_{0.9}Fe_{0.1}O_{3-\delta}$ (▲, $T_s = 973$; ◆, $T_s = 1373$ K) samples in the temperature range 773–973 K

Table 4 Band gap values for the the $KTaO_3$ and $KTa_{0.9}Fe_{0.1}O_{3-\delta}$ oxide powders

Sample	T_s (K)	E_{gap} (eV)
$KTaO_3$	973	1.8
$KTaO_3$	1373	2.5
$KTa_{0.9}Fe_{0.1}O_{3-\delta}$	973	2.5
$KTa_{0.9}Fe_{0.1}O_{3-\delta}$	1373	2.5

1 mol dm^{-3} KOH using cyclic voltammetry. Figure 5 shows representative voltammetric curves for the Fe/$KTa_{0.9}Fe_{0.1}O_{3-\delta}$ electrode synthesized at 973 K and the Fe support. Similar curves were obtained for the oxide synthesized at 1373 K. The voltammetric profile is rather featureless, showing a wide plateau region where only non-Faradaic current flows. It is clear that the coated perovskite electrode presents a wider range of electrochemical stability and higher current intensity than the iron substrate, as the inset shows.

The electrochemical active surface area of the oxide coating was estimated from the dependence of the non-Faradaic currents on the sweep rate obtained in the potential range –0.20 to +0.20 V vs. Ag/AgCl (Fig. 6a). A good linear relationship is observed for sweep rates ≤ 10 mV s^{-1} (correlation coefficients of the order of 0.998), although a deviation from linearity is detected for higher sweep rates, as Fig. 6b reveals. This deviation is due to ohmic drop, mainly to the oxide resistivity and evident on the voltammetric curves when the sweep is reversed. The observed sluggish current switching, with a rise time of several seconds, is associated with the time constant of the series combination of the electrode capacitance and the ohmic resistance of the oxide [8, 14]. The latter value is very high, as expected from the oxide electrical resistivity data.

From the slope of the linear region of the plot of double layer charging current versus sweep rate, the capacitance of the oxide|solution interface ($C = dq/dE = dI/dv$) was calculated. A value of 302 ± 60 μF cm^{-2} was obtained. An electrode roughness factor of 5 ± 1 was estimated by assuming the value of 60 μF cm^{-2} for the capacitance of a smooth oxide surface [15]. Values in the range of 100–1000 were obtained by Bockris and Otagawa [6] for a large set of substituted pelleted perovskite electrodes containing first-row transition metal ions. Singh et al. [16] reported even higher values for $LaNiO_3$-substituted Ni-coated electrodes. The difference between the data can be attributed to the oxide composition and preparation method and/or to the type of electrode used.

In order to test the electrode stability, charging currents were recorded after the electrodes had been used for oxygen evolution. No appreciable changes were observed in the roughness factors, leading us to conclude that the electrodes are stable under oxygen evolution conditions in alkaline medium.

Oxygen evolution reaction

The Fe/$KTa_{0.9}Fe_{0.1}O_{3-\delta}$ electrode was tested as a possible anode material for oxygen evolution in alkaline medium, described by the equation:

$$4OH^- \rightarrow O_2 + 2H_2O + 4e^- \quad (1)$$

Steady state polarization curves were obtained after stabilizing the electrode at 700 mV for 15 min, in order to obtain a stable surface, prior to the measurements. Measurements were recorded from the higher to the lower potential value.

Figure 7 presents a polarization curve obtained in the potential range from 0.000 to 0.600 V vs. Ag/AgCl at a sweep rate of 0.5 mV s^{-1} and the corresponding Tafel representation is illustrated in Fig. 8. A deviation from the Tafel behaviour, due to ohmic drop, is clearly seen

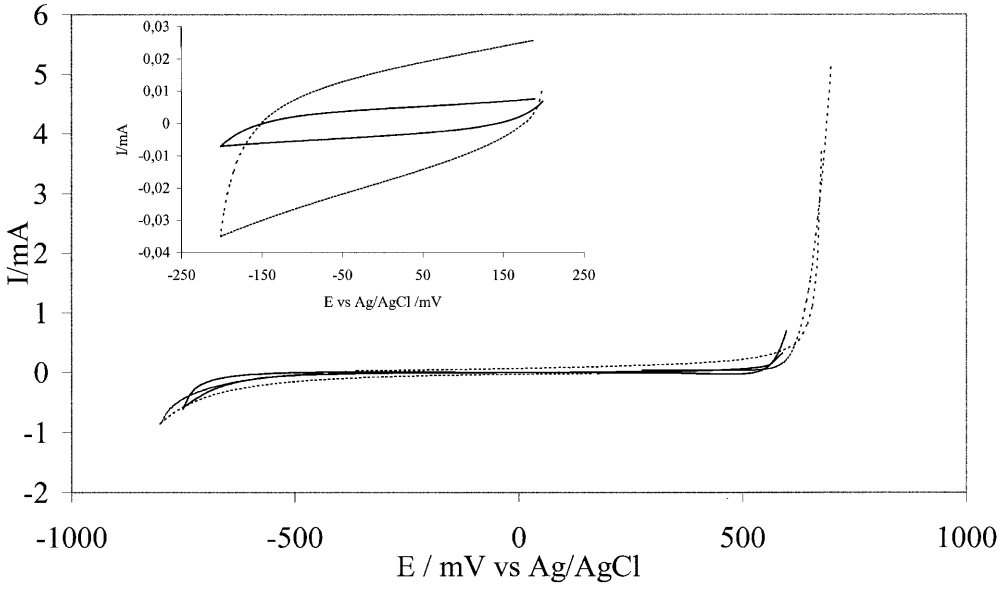

Fig. 5 Cyclic voltammograms for iron (*solid line*) and $KTa_{0.9}Fe_{0.1}O_{3-\delta}$ (*broken line*) iron-coated electrodes in 1 mol dm^{-3} KOH. Sweep rate 20 mV s^{-1}; electrode geometric area 1.3 cm^2. *Inset*: enlargement of the potential interval near 0.00 V vs. Ag/AgCl

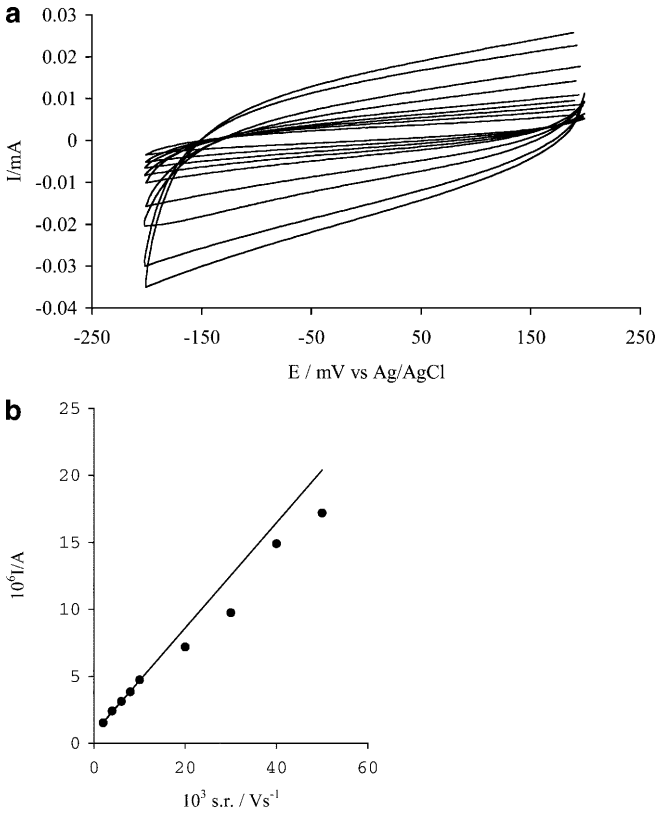

Fig. 6 **a** Cyclic voltammograms obtained in the double layer region and **b** double layer charging current as a function of sweep rate, for an iron-coated perovskite $KTa_{0.9}Fe_{0.1}O_{3-\delta}$ electrode at 0.000 V vs. Ag/AgCl, in 1 mol dm^{-3} KOH. Sweep rates 2, 4, 6, 8, 10, 20, 30, 40 and 50 mV s^{-1}; electrode geometric area 1.3 cm^2

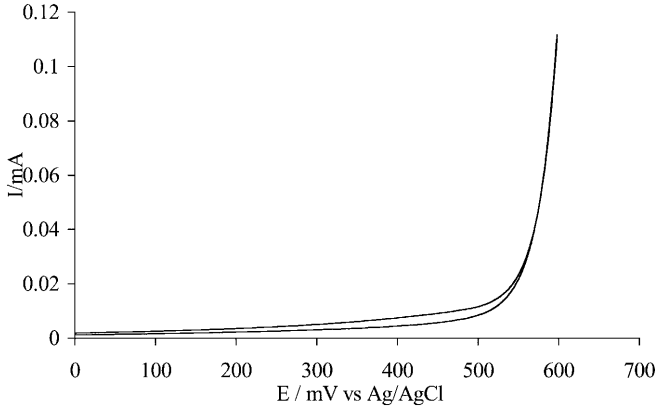

Fig. 7 Polarization curve obtained at a sweep rate of 0.5 mV s^{-1} for an iron-coated $KTa_{0.9}Fe_{0.1}O_{3-\delta}$ perovskite electrode in 1 mol dm^{-3} KOH

for high potentials. The ohmic drop was estimated indirectly by first drawing the low-potential Tafel line up to the highest current density and then measuring the ΔE at constant current density between the experimental points and the extended line [17]. The plot of ΔE vs. j is linear, as the inset shows. Ohmic drops of the order of 11 Ω were estimated. This relatively high value is mainly due to oxide resistivity.

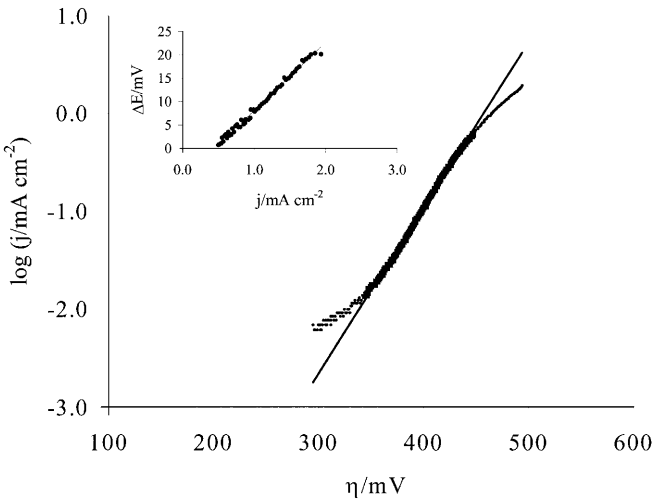

Fig. 8 Tafel representation for oxygen evolution on an iron-coated $KTa_{0.9}Fe_{0.1}O_{3-\delta}$ perovskite electrode in 1 mol dm^{-3} KOH. Current normalized considering the geometric area. *Inset*: ΔE at constant current between the experimental points and the extended straight line versus the current density

The Tafel representations show a single Tafel region, with a Tafel slope of 59 ± 1 mV and an exchange current density of 1.8×10^{-11} A cm^{-2}. Tafel slopes ranging from 60 to 130 mV are reported for perovskite electrodes, depending on the oxide composition, preparation method and electrode type [5, 10, 16, 18, 19, 20]. The value obtained for the $Fe/KTa_{0.9}Fe_{0.1}O_{3-\delta}$ electrode is similar to those published by Singh et al. [16] for coated perovskite electrodes and by Bockris and Otagawa [5] for ceramic pellet electrodes.

According to the mechanism proposed by Bockris et al. [4, 5, 6, 21] for oxygen evolution on perovskite oxides, the 60 mV Tafel slope is consistent with the adsorption of OH_{ads} intermediates on the transition metal atoms, following a Temkin isotherm for coverage of $0.2 < \theta < 0.8$. The transition metal atoms act as adsorption sites at the perovskite surface, the rate determining step being the electrochemical desorption of the OH_{ads} intermediates according to:

$$M^z - OH + OH^- \rightarrow M^Z...H_2{}'O_2 + e^- \qquad (2)$$

Conclusions

In this work we have synthesized single-phase $KTa_{0.9}Fe_{0.1}O_{3-\delta}$ oxide powders with a cubic perovskite structure and attempted to study those properties which are relevant to its application as an electrode material. The results have shown that it is possible to fabricate stable $Fe/KTa_{0.9}Fe_{0.1}O_{3-\delta}$ coated electrodes suitable to evolve oxygen.

Acknowledgements Financial support of the programme PRAXIS XXI (project 435 PRAXIS/PCEX/C/QUI/83/96) from the Ministério da Ciência e Tecnologia is acknowledged.

References

1. Kato H, Kudo A (1999) Catal Lett 58:153
2. Ellis AB, Kaiser SW, Wrigton MS (1976) J Phys Chem 80:1325
3. Vousden P (1951) Acta Crystallogr 4:313
4. Khang D, Wemple SH (1965) J Appl Phys 36:2925
5. JO'M Bockris, Otagawa T (1983) J Phys Chem 87:2963
6. JO'M Bockris, Otagawa T (1984) J Electrochem Soc 131:290
7. JO'M Bockris, Otagawa T, Young V (1983) J Electroanal Chem 150:633
8. da Silva Pereira MI, Melo MJBV, Costa FMA, Nunes MR, Peter LM (1989) J Chem Soc Faraday Trans 1 85:2473
9. Larramona G, Gutierrez C, da Silva Pereira MI, Nunes MR, Costa FMA (1989) J Chem Soc Faraday Trans 1 85:907
10. Tomás HM, Tavares AC, da Silva Pereira MI, Nunes MR, Costa FMA (1992) J Chem Soc Faraday Trans 1 88:2517
11. Scherban T, Nowick AS, Boatner LA, Abraham MM (1992) Appl Phys A 55:324
12. Tiwari SK, Singh SP, Singh RN (1996) J Electrochem Soc 143:1505
13. Lee W-K, Nowick AS, Boatner LA (1986) Solid State Ionics 18/19:989
14. Ciriaco MLF, da Silva Pereira MI, Nunes MR, Costa FM (1999) Port Electrochim Acta 17:149
15. Levine S, Smith A, (1971) Discuss Faraday Soc 52:290
16. Singh RN, Tiwari SK, Sharma T, Chartier P, Koenig JF (1999) J New Mater Electrochem Syst 2:65
17. Boodts JCF, Trasatti S (1989) J Appl Electrochem 19:255
18. Kinoshita K (1992) Electrochemical oxygen technology. (Electrochemical Society series) Wiley, New York
19. Wattiaux A, Grenier JC, Pouchard M, Hagenmuller P (1987) J Electrochem Soc 134:1715
20. Matsumoto Y, Kurimoto J, Sato E (1980) Electrochim Acta 25:539
21. JO'M Bockris, Khan Shahed UM (1993) Surface electrochemistry. Plenum Press, New York